Hemp Hurd and Alfalfa as Particle Filler to Improve the Thermo-Mechanical and Fire Retardant Properties of Poly(3-Hydroxybutyrate-Co-3-Hydroxyhexanoate)

Hemp hurd and alfalfa as particle filler to improve the thermo-mechanical and fire retardant properties of poly(3-hydroxybutyrate-co-3-hydroxyhexanoate)

Daniele Battegazzore*, Amir Noori, Alberto Frache

Dipartimento di Scienza Applicata e Tecnologia, Politecnico di Torino, Alessandria site

Viale Teresa Michel 5, 15121 Alessandria, Italy

*Corresponding author: Tel/Fax: +390131229343/+390131229399; e-mail address:

daniele.battegazzore@polito.it

Abstract

The poor thermo-mechanical and flame-retardant properties of biopolymers are currently limiting their application and potential exploitation as sustainable polymers. The use of agricultural by-products as a functional filler for biopolymers is here presented to address the production of environmentally friendly and economically sustainable biocomposites. To this aim, hemp hurd and alfalfa particles were melt-blended with a PHB co-polymer. The 30 wt.% of filler achieves an improvement of 150% in stiffness. The same composites show an increase in the heat deflection temperature over 100°C. Flame retardant properties were also evaluated evidencing strong reductions in flame spread rates (-40%) and combustion kinetics (-30%). The achieved performances are compared with those reported in the literature for PHB composites pointing out how these completely renewable materials can compete with other currently studied solutions. The new presented composites show an opportunity for the production of functional and sustainable materials through the valorization of agricultural by-products.

1. Introduction

Hemp is a multi-purpose crop delivering fiber, shive and seed. The high added-value product in the hemp chain is the fiber production used for paper, insulation material and composites. The shive or hurd, the woody inner core of the stem constitutes 60 wt.-% of the original plant [1]. Hemp seeds have a high nutritional value and are also used to extract hemp oil. Both seeds and oil are used for human food and animal feed [1]. Hemp hurd is used as animal bedding for approximately 95% and in concrete-like blocks as an insulating material for construction for the remaining 5% [2]. Such blocks are not structural elements but are usable as a replacement for wood. The use of hurd, one of the secondary products (by-product) from the hemp chain, is at the center of this article.

Alfalfa is a perennial herbaceous legume, widely grown throughout the world that it is mainly used as feed for domestic animals. It accounts for a US production around 57 million tons in 2013 [3]. In the same year, Italy was the third worldwide exporter in terms of quantity with more than 200 thousand tons (data from FAO [3]). Unfortunately, the overproduction of alfalfa leads to the collapse of the price and, consequently, to the impossibility of handling and selling this material. A second opportunity for its use is therefore necessary to avoid wasting.

One of the possible options for using these by-products is the incorporation into a polymer matrix. Indeed, organic natural fillers can be renewable, biodegradable and cheaper alternatives to synthetic or inorganic ones [4]. They have been extensively studied both in fossil-based matrices or bio-based ones in recent times for different applicative fields [5-9]. However, from an environmental point of view, the best solution is to use bio-based and biodegradable matrices [10-12]. In this scenario, PLA has already been investigated by achieving balanced mechanical properties between stiffness and toughness [13-15]. Unfortunately, PLA has an important limitation in the application when the temperatures are over the T_g. For this reason, the use of another biodegradable material was investigated in this article, namely a commercial grade of poly(3-hydroxybutyrate-co-3-hydroxyhexanoate).

The selected processing method is the most widely used to mix a filler with a polymer in a melt state: the co-rotating twin screw extrusion. It allows fast and continuous processing and a final pelletisation of the composite material.

Furthermore, it is generally characterized by a modular screw design to yield distribution and dispersion of fillers, but the high amounts of shear induced in the process can dramatically damage the aspect ratio of the fillers. Fiber and particle loadings up to 70 wt.-% have been achieved [16]; however, at these high loadings the processing is difficult and the surface appearance is deteriorated. For these reasons, 20–50 wt.-% loadings are more common. In this research 30 wt.-% has been used.

One of the established markets for composites with natural fillers is their molding into panels for automotive interior applications such as door panels/inserts, trunk liners, spare wheel covers, parcel trays, headliners, columns and much more [17] or partial replacement of wooden part in furniture [18,19]. Several researchers have worked with fibers for developing thermoplastic and thermoset composites [20-29]. Only a few researches have been done with bioplastics and even less with PHB [30-33].

Although the field seems promising, there is not enough data to hypothesize a possible industrial exploitation as transferring from a laboratory scale to a semi-industrial one. For this reason, in this paper a commercial grade PHB was melt mixed together with two natural by-products by using a semi-industrial extruder. Then the resulting pellets were processed by compression or injection molding and characterized for thermo-mechanical properties. Furthermore, all the vegetal compounds, the matrix and their derived composites are flammables, thus this behavior is a crucial aspect that should be well known and improved for an industrial application in buildings or means of transport. Hence, the combustion properties of the resultant materials have been investigated by a cone calorimeter under a 35 kW/m^2 heat flux, mimicking the conditions of a real scenario in developing fire conditions. As the

results show, the char formation during the burning of the bio-based fillers gave advantages to the flame behavior of the whole composite.

Moreover, horizontal burning test UL94 HB was also investigated to evaluate the dripping of flaming polymer onto underlying materials that may promote the propagation of fire or the formation of a char layer. The latter leads to a reduction in the burning rate (BR) of the polymer and dripping. Finally, also the LOI test in vertical conformation confirms the reduction in the combustion speed and the non-dripping behavior, even if the LOI value found for the composites is significantly lower than the neat matrix.

2. Materials and methods

2.1 Materials

Poly(3-hydroxybutyrate-co-3-hydroxyhexanoate) (PHB) was supplied by Kaneka Cooperation (AONILEX X131A grade). Hemp Hurd in the forms of Chips (hereafter abbreviated as HHC) was provided by the local hemp association (AssoCanapa). HHC has the parallelepiped shape with lengths between 300 and 5000 μm. Alfalfa (AA) was supplied by a local farm and ground to reach particle size lower than 5mm. AA is a heterogeneous mixture of fibers till 3 mm length and more spherical particles from 0.2 to 1 mm.

Both polymer and fillers were dried at 80 and 100°C respectively, for 6 hours in an industrial dryer (Piovan HR50 model) before compounding.

2.2 PHB-based composite preparation

30 wt.-% of filler content was mixed with PHB through a lab-scale co-rotating twin screw extruder LEISTRITZ ZSE 18/40 D. The screw speed was fixed at 250 rpm. The heating temperature was set in

the eight thermostated barrel blocks from 145 to 160°C (Figure S1 in the Supporting Info). The compounding output was fixed at 1.7 kg/h. The pellets obtained by compounding were dried at 80°C for 4 h in an industrial dryer Piovan HR50 model before the injection molding process.

The specimens for dynamic-mechanical thermal analyses (DMTA) were prepared by using a hot compression molding press at 160°C and 10 MPa for 3 min obtaining 60x60x1 mm^3 plates. The 6x30x1 mm^3 specimens for tests were derived from plates by razor blade cutting.

The specimens for cone calorimeter, UL94 and LOI were prepared by using a hot compression molding press at 160°C and 10 MPa for 3 min with a specific mold.

The injection molding machine Babyplast 6/10P was used to prepare the 5A type specimens according to the standard ISO527 for tension tests.

The names of the samples have been coded on the basis of the weight composition and the filler type: PHB30HHC and PHB30AA representing the composite loaded with 30 wt.-% of Hemp Hurd Chips and Alfalfa, respectively.

2.3 Characterization techniques

The Scanning Electron Microscope (SEM) magnifications were taken with LEO 1400 VP Series (beam voltage: 20 kV; WD: 15mm) on the fractured cross sections. The samples were sputtered with gold.

The Differential Scanning Calorimetry (DSC) analyses were done on a DSC Q20 (TA Instruments). The samples (about 8 mg) were heated at 10°C/min under nitrogen from 0°C to 200°C. The percentage crystallinity (X_c) of neat polymer and composites was calculated using **Equation 1**.

$$\chi_c(\%) = \frac{\Delta H_m - \Delta H_{cc}}{\Delta H_{100}(1-x)} * 100$$

Equation 1

where ΔH_m *and* ΔH_{cc} are the melting and cold crystallization enthalpies obtained from the heating scan, ΔH_{100} is the melting enthalpy of the 100% crystalline polymer matrix (164 J/g for PHB [34]) and x is the filler weight percentage.

The Dynamic Mechanical Thermal Analysis (DMTA) was performed using a DMA Q800 (TA Instruments). A temperature range from 30 to 120 ºC in air, a heating rate of 3 ºC/min, a 1 Hz frequency and a 0.05% of oscillation amplitude in strain-controlled mode were adopted and the storage modulus (E') was measured. The tension film or the dual cantilever clamp were used. For each formulation, the test was repeated two times and the experimental error was calculated as the standard deviation for all the measured parameters.

Tensile tests on 5A type specimens were performed at room temperature (23±1°C) using a Zwick Roell Z100 machine, following the ISO 527 standard. A loading cell of 5 kN and a rate of 1 mm/min was used to calculate the tensile modulus, subsequently, the rate was increased up to 5 mm/min until the specimen broke. Ten specimens were used for each formulation and the average values and corresponding standard deviations were calculated. These tests provided Young's modulus values (E), elongation at break (ε), and maximum tensile strength (σ_{max}) of the biocomposites.

The rheological properties of composites were measured using an ARES rheometer fitted with a 25 mm parallel plate geometry. Tests were performed at 160°C under a nitrogen atmosphere to avoid any degradation. The sample disks for the rheometer were compression molded at the same temperature into a 25 mm diameter hole and 1 mm thick plate. Dynamic strain sweep tests were carried out and confirmed the linearity of the viscoelastic region up to 20% strain at 62.8 rad/s of frequency. Furthermore, the frequency sweeps were carried out to determine the complex viscosity (η*) over the frequency range of 0.1–100 rad/s at 10% of strain.

The cone calorimeter tests (Fire Testing Technology, FTT) were performed according to the ISO 5660 standard [35] on 100 x 100 x 1.5 mm^3 specimens. The samples were exposed to 35 kW/m^2 heat flux in

the horizontal configuration in an aluminum tray. The test was repeated three times for each formulation and the standard deviation was calculated as the experimental error for all measured parameters. The Time to Ignition (TTI, s), Total Heat Release (THR, MJ/m^2), Peak of Heat Release Rate (PHRR, kW/m^2), Total Smoke Release (TSR, m^2/m^2) and final residue (%) were assessed.

The horizontal burning test following UL94 HB (ASTM D635 and ISO 1210) procedure was repeated on 4 self-supporting bars specimens (12 x 100 x 3 mm^3) in order to evaluate the linear burning rate (BR) or the time of burning. Each sample was marked at 20 mm and 80 mm from one end of the test specimen. A flame with a 20 mm high blue cone was applied at 45° from horizontal for 30 s or the time to reach the 20 mm mark. When the flame passes the 20 mm and 80 mm mark, the burning time was recorded and the BR (mm/min) was calculated.

The limiting oxygen index (LOI) was calculated according to the standard ASTM D2863 with test specimen type IV. The test measures the minimum concentration of oxygen that is required to support flaming combustion of a material in a flowing mixture of oxygen and nitrogen.

All the samples were conditioned at 23±1 °C and 50% R.H., in a climate-controlled chamber Binder BFK240 for a minimum of 3 days, till a stable weight was reached.

2.4 Micromechanical modelling

To predict and analyze yield stress, the most often applied correlation is attributed to Nicolais and Narkis [36]. They assumed that the filler decreases the effective cross-section of the matrix which carries the load during deformation. The model does not take into consideration the effect of stress concentrations, assumes zero filler-matrix interaction and ignores all other factors influencing the yield stress.

For this reason, another model that takes into account at least some of the factors neglected by Nicolais and Narkis is used. The model from Pukanszky [37] applies a different expression for the effective

load-bearing cross-section [38] and considers also the influence of interfacial interaction and interphase formation. The **Equation 2** [37,39] allows to investigate the linear relationship between the natural logarithm of reduced yield stress σ_{red} and the filler content [40,41].

$$\log(\sigma_{red}) = \log \frac{\sigma_c \cdot (1 + 2.5 \cdot \varphi_f)}{\sigma_m \cdot (1 - \varphi_f)} = B \cdot \varphi_f$$

Equation 2

where σ_c and σ_m are the yield stresses (σ_y) of the composite and matrix, respectively; B is a term corresponding to the load carrying capability of the filler and depends on filler-matrix interactions; and ϕ_f is the filler volumetric fraction within the polymer matrix.

The volumetric fraction (ϕ) is determined from the weight fractions calculated using the density of each component.

3. Result and discussion

3.1 Evaluation of the fillers dimensions and adhesion with SEM

The morphology and elemental analysis of the fillers have been already reported in a previous article [42]. The chopped natural by-products show a broad range of dimensions and aspect ratio reported in Figure 1.

By processing, the screw profile made of conveying, kneading and mixing elements causes intense shearing that results in solids breakup and dispersive mixing.

In this context, SEM is used to investigate the dimension reduction of the filler particles. To study this aspect, the method of matrix dissolution in chloroform and evaluation of the filler particle sizes from SEM magnifications is used. The length size distribution and the aspect ratio of the particles are reported in Figure 1.

Despite the difference in the starting dimensions of the two fillers, after the extrusion process, the particles are reduced to similar dimensions. Indeed, Figure 1 reports the highest statistical frequency (40-50%) for both HHC and AA in the sampling between 250 and 500 μm and over 90% of the particle size falls between 100 μm and 1 mm. Therefore, the dominant factors are the process conditions (screw profile, screw velocity, output).

As far as aspect ratio (a.r.) is considered, the smallest aspect ratio (1-2) is found for over 35% of the particles and the cumulative distribution up to 5 covers around 90%. Also in this case, the a.r. is reduced in a similar way in the two fillers (e.g. the HHC had 25% of fibers with a.r.>10 that completely disappeared after extrusion).

SEM was used also to investigate the morphology of the PHB-based composites on the cross- section fractures in order to visually evaluate the filler dispersion and the filler-matrix adhesion. Figure 2 reports SEM micrographs of PHB loaded with hemp hurd chips (a) and alfalfa (b). From such magnifications, fillers pull-out and breakage out of the matrix plane reveal the not perfect adhesion between filler and matrix; nevertheless, there is no segregation or filler free part in the fracture surfaces, thus the dispersion seems good.

3.2 Crystallinity of the composites

The study on the crystallinity of the materials has been performed with DSC analyses directly on the samples molded for the mechanical tests in order to verify any changes in crystallinity that could affect such properties. Indeed, the natural particles can act as nucleating agent and influence the polymer crystallization mechanism. This process has already been reported many times in the literature also with the same fillers used in this research [42].

From the reported data in Table 1, no significant changes were recorded in the first heating run, indeed the crystallinity percentage slightly increased only from 31 to 35% in the case of AA. Therefore, the mechanical and thermo-mechanical properties are mainly regardless of crystallinity.

The nucleating effect that is attributed to the presence of natural fillers is therefore extremely reduced in the case of PHB, an already highly crystalline polymer.

3.3 Thermo-mechanical properties

Figure 3a illustrates the storage modulus of composites versus temperature. PHB does not present a glass transition in the studied temperature range, thus the modulus decrease associated with the increase of temperature is more gradual than PLA. Indeed, E' goes from 1.42 GPa at 30°C to 0.28 GPa at 120°C. The HDT which is defined as the temperature at which the material achieves a modulus of 800 MPa (dotted line in Figure 3a), following Takemori calculation [43], was determined at 67°C.

An increase of E' has been observed for the composites across the whole studied temperature range with a gradual reduction on heating (Figure 3a).

HHC has proven to be the most efficient filler for enhancing the thermo-mechanical behavior of PHB-based composites such as increasing the HDT value to 113°C (Table 1). A great improvement was also reached with AA in which the HDT point was around 102°C (Table 1).

Considering PHB-based composites with natural fillers, Singh et al. [44] have reported an increase of 24°C in HDT for composite with 40 wt.-% of wood fiber compared to neat PHBV. This literature result is significantly lower than what is found in the worst case of the present research (+35°C for AA), even with a lower filler amount (30 wt.-%).

The surprising thermo-mechanical enhancements which were obtained for both HHC and AA composites, widely increase the opportunities for their employment in applications above room temperature.

3.4. Tension tests and adhesion analyses from mechanical data

The representative curves of the tensile tests are plotted in Figure 3b and related data are reported in Table 2.

Neat PHB exhibits a maximum stress of 27.5 MPa at a deformation of 6.2%. The addition of 30 wt.-% filler significantly lowers the maximum stress and elongation. As expected from the DMTA analysis the best tensile modulus and strength were achieved with HHC filler (Table 2).

The increasing trend of modulus as a function of the volumetric fraction ϕ was plotted in Figure 4a and compared with other biocomposites found in the literature. Despite the fact that a comparison of the results with the literature is not easy because of the wide variety of PHB grades (different type and amount of copolymer), the best results in modulus increase were achieved with fibers such as jute [45], kenaf [30] and pineapple leaf long fiber [31]. Even two by-products such as corn straws and wheat straws have been used with surprising improvements in the modulus [46]. This important achievement is probably due to the high fibrous content of these by-products. Similar results to the ones obtained with HHC and AA have been reported with soy stalks [46], wood [30,44], cellulose [45,47], flax [33,48] and abaca fibers [45]. There are also cases with low modulus enhancement, as reported by Coats et al. with wood particles [49].

Stiffness does not depend so much on the interfacial adhesion between filler and matrix, and the aspect ratio of the filler, but tensile strength and elongation strongly do.

As far as composite tensile strength is concerned, if there is no long fiber present but mainly particle like shapes (aspect ratio 1-2), the filler weakens the material rather than strengthens it and composite failure is controlled by the matrix. This trend has already been reported many times by other authors [30,33,44,46,48,49] and verified also in the present research (Table 2). To compare the various results,

it was chosen to exploit the model from Pukanszky [37] that takes into account also the influence of interfacial interaction and interphase formation (Equation 2 [37,39]).

Figure 4b plots the natural logarithm of reduced yield stress (σ_{red}) as a function of the filler content (Φ) as well as the calculated B factor for the PHB-based composites.

The highest B value of 2.25 and therefore the best stress transfer between filler and matrix is achieved with HHC. This result is completely comparable with what is found in the literature for composites with wood, stalks and straws [30,33,44,46,49] (full filled marker in Figure 4b). Better results are obtainable only by means of fibers (void and crossed marker in Figure 4b) which probably have a greater aspect ratio and consequently yield a composite failure controlled by the fiber. These kinds of fibers are generally primary products; they cannot be determined either as by-products or wastes similar to those examined in this article.

A concluding comment on the elongation and supposed impact performances must be highlighted as the ultimate use occurs in the automotive industry. The elongation is extremely limited, with a 76% reduction compared to the PHB matrix. This is an expected trend reported in the literature [50]. An initial rough evaluation of impact performances could be supposed given the energy absorbed during the tensile test from the area under the stress strain curves. Thus, the areas of the composites are conspicuously less extensive than that of the matrix, with a reduction of approximately 80%. This behavior can constitute a limitation in several applications. A possible improvement of the elongation and impact properties could be achieved with filler surface treatments or by the addition of an adhesion promoter additive [19,51-54]. As expected, these treatments involve an increase in the costs and the possibility of a no longer biodegradable composite.

3.5 Rheology

The viscoelastic response of neat PHB and PHB-based biocomposites was investigated in order to evaluate the effect of the fillers on PHB melt rheology. The viscosity of the system is extremely important for the processability of the composites.

Figure 5 displays the logarithmic dependence of complex viscosity (η*) versus the angular frequency. Neat PHB approached a constant value in the Newtonian plateau at low frequencies (1170 Pa*s). The two composites exhibited a higher viscosity than neat PHB all over the investigated frequency range (12000 Pa*s and 7800 Pa*s at 0.1 rad/s for HHC and AA composites, respectively). These results can be explained in terms of restricted mobility of the polymer melt due to the interaction between the polymer chains and filler particles in the melt [55]. Furthermore, these results are important for the other three aspects: first, they exclude an extensive degradation of the matrix during the processing since the viscosity is increased. Second, they show that such an increase is not excessive enough to preclude the use in other shaping processes such as injection molding, even if this variation has to be carefully considered. Indeed at 100 rad/s the complex viscosity pass from 340 Pa*s of the neat PHB to 1500-1900 Pa*s of the composites. The last, the increased melt viscosity prevents dripping during the flame. It can moreover either trap or slow down volatilization and the evolution of degradation products. In addition to that, the aforementioned viscosity promotes char formation as an protective layer [56].

3.6 Combustion tests by cone calorimetry, UL94 HB and LOI

The use of natural composites in the transportation, building and furniture industries raised up the important aspect of flammability. To examine such an important parameter, the cone calorimeter under a 35 kW/m^2 heat flux and UL94 in horizontal configuration were used. Table 3 summarizes the

collected data and Figure 6 illustrates one representative curve of the HRR at the cone test and two pictures of the UL 94 test for each formulation.

Both composites exhibited a similar behavior: they ignite in 30 s with an anticipation with respect to the neat matrix and immediately spread the fire. They reach quite rapidly the PHRR (487 and 478 kW/m^2 for AA and HHC, respectively) that is more than 30% lower than the neat PHB (714 kW/m^2). Similar TTI anticipation and PHHR reduction occurred in PP composites reinforced with lignocellulosic fibers [57]. HRR is believed to have the greatest influence on the fire hazard [58] but the contemporary decrease in the TTI gave a contrasting result. For this reason, a fire index has been introduced to assess the hazard of developing fires into a single number, namely FIGRA (fire growth rate = PHRR/time to PHRR) [58]. The data reported in Table 3 show the slight reduction of FIGRA by adding the fillers to PHB and thus the effectiveness of such additives to limit the fire spread. As already reported bio-based compounds could give important advantages as flame retardant additives for their ability to form thermally stable charred residues which act as an insulator for the under layers [59]. Moreover, the further use of common flame retardants in the formulation could even more enhance such property [60].

Analyzing the other data from the cone tests and considering the experimental error, THR values in Table 3 are almost equal for all the formulations (40 MJ/m^2). On the other hand, the presence of fillers promotes the formation of a thermally stable residue mainly due to the fillers themselves, as it is visible by comparing the data in Table 3 (7.8 % and 6.5 % *vs*. 0 % for PHB30AA, PHB30HHC and PHB, respectively). The difference in the residue quantity of PHB30AA and PHB30HHC is due to the chemical composition of HHC and AA leaving a different residue after combustion, as previously reported [42].

It is well known that the THR strongly depends on the total mass loss (the difference between the specimen mass and char yield) [58]. Despite the presence of residue, the THR was not reduced because

the initial mass of the composite samples was 10-15% higher than those of the neat PHB (see Table 3). Therefore, the amount of combusted material is similar or even higher when fillers are introduced, bringing THR to the similar values.

Continuing to explore the registered data from cone tests, the fillers are also responsible for the increase in the total released smoke which is reported in the TSR column in Table 3. This fact is likely due to the incomplete combustion generated by the introduction of the fillers. Indeed, the presence of lignin or other compounds in the fillers causes the contemporaneous formation of char and volatiles from cellulose [61,62].

In the cone calorimetry, the specimen is mounted horizontally, eliminating some physical effects in the combustion such as dripping. Conversely, in the UL 94 test a withdraw of the polymer from the fire source could occur.

The more viscous melt of composites presents limited tendency to drip, keeping the polymer in place to feed the flame (Figure 6). However, the char formed at the surface of the burning sample in UL 94 tests is not effective enough to stop the flame and the sample continues to burn but more slowly (Figure 6 and Table 3).

The same speed reduction is observable in the LOI test where the sample is burned in a vertical position. The behavior of the neat PHB is completely different from the composites. Indeed, the neat matrix has a dripping of the molten material along the walls of the sample that rapidly reaches the base of the sample. At times, these drops get burnt. In the first case, the flame is brought to the sign which is located 5cm below the sample top and subsequently leads to a no-pass state in the LOI classification. In the second instance, the combustible material drips down from the top and the flame extinguishes, resulting in the success of the test. Conversely, the composites are consumed gradually without dripping; thus, the extinguishing is more reproducible.

According to the standard, the LOI value is reduced by the presence of natural fillers from 23.9% of the PHB to 20.8% and 20.1% of PHB30AA and PHB30HHC, respectively. Similar LOI results for composites were obtained with PP and natural fillers [63,64]. Generally, the LOI of natural fiber is higher than that of common polymer, suggesting that natural fibers may be easier to extinguish in a fire than polymers [65]. On the other hand, cotton has a LOI of 18-20 and a high content of cellulose tends to increase the flammability of the fiber [64]. Indeed, the HHC filler, which is suspect for having more cellulosic portion, has a lower LOI than AA. From the cone calorimeter and UL94 tests, the addition of such by-products does not worsen the burning behavior of the material despite being flammable materials. Conversely, they bring a modest flame retardant contribution. Obviously, in an application linked to the building or transport sector, it will be necessary to combine a flame retardant [61].

4. Conclusions

Two renewable materials as hemp hurd (HHC) and alfalfa (AA) were taken into consideration for the direct use as filler in poly(3-hydroxybutyrate-co-3-hydroxyhexanoate) (PHB). The analysis of the particle size after the melt mixing showed similar distribution despite the fact that the initial values were different due to grinding action of the processing and screw profile.

DMTA has shown a huge increase of HDT of the materials that raised to 113°C and 102°C with HHC and AA, respectively. This important finding widens the application in temperature of such bioplastic. Tension tests on injection molded specimens were performed, revealing balanced properties between stiffness (+150%) and toughness (-20%). Moreover, these tests gave the opportunity to analyze the adhesion/stress transfer between the matrix and the fillers. Indeed, considering that the crystallinity did not change in the matrix and the filler was mainly in particle form (aspect ratio 1-3), by applying the equation of Pukanszky to the composite strengths, the B value reflects the filler-matrix interaction. A direct comparison between HHC and AA shows the highest value of 2.25 was achieved with HHC that

is comparable with other results obtained in the literature with wood, stalks and straws. Both composites exhibited a similar behavior to heat exposure (35 kW/m^2) with a 30% reduction of the peak of heat release rate with respect to the neat PHB. Moreover, the variation in the melt viscosity changes the behavior at UL 94 HB and LOI test sensibly decreasing the burning rate with respect to the neat polymer.

The thermo-mechanical results, as well as the fire properties linked to the use of semi-industrial equipment, lay the basis for future improvements in the composite industrialization in order to obtain an environmental and economic sustainable composite.

Acknowledgments

The authors would like to thank Mrs Giuseppina Iacono for SEM analyses and Dr Alberto Cisternino for the compounding trials.

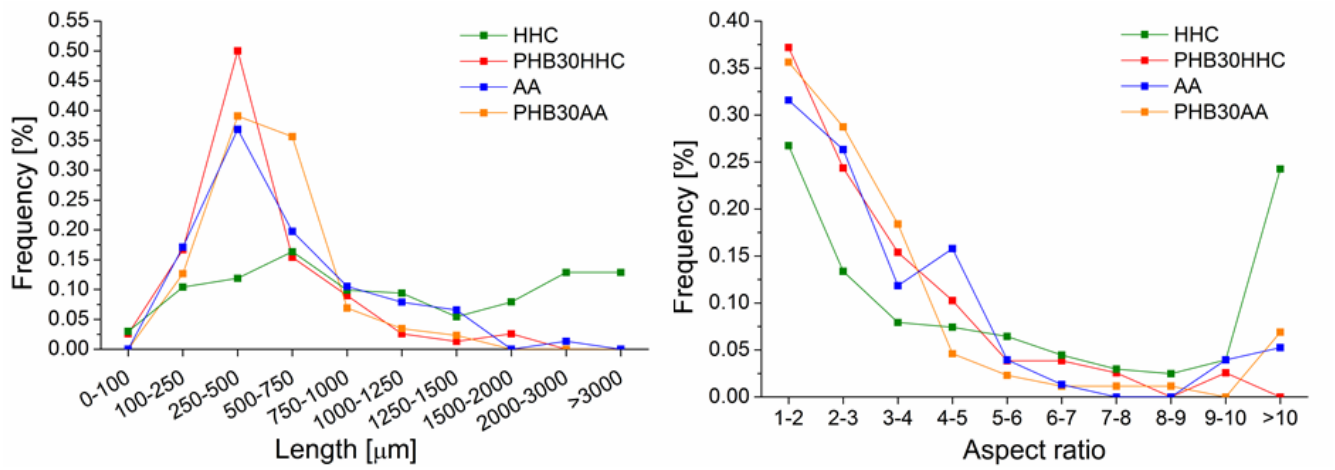

FIG. 1. Length size and a. r. distribution of the HHC and AA particles before processing and extracted from the PHB-based processed formulations.

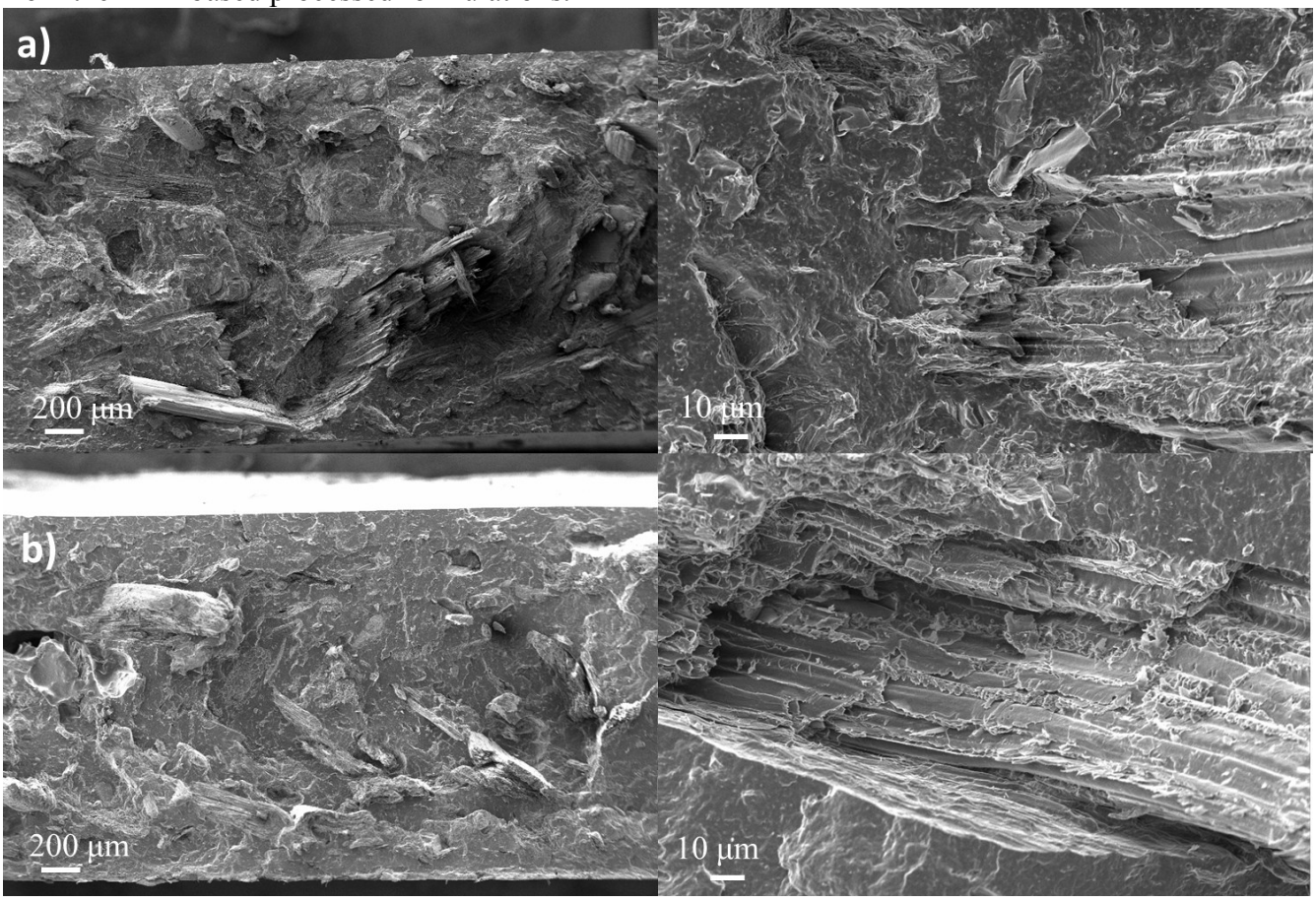

FIG. 2. SEM magnifications of PHB loaded with AA (a) and HHC (b).

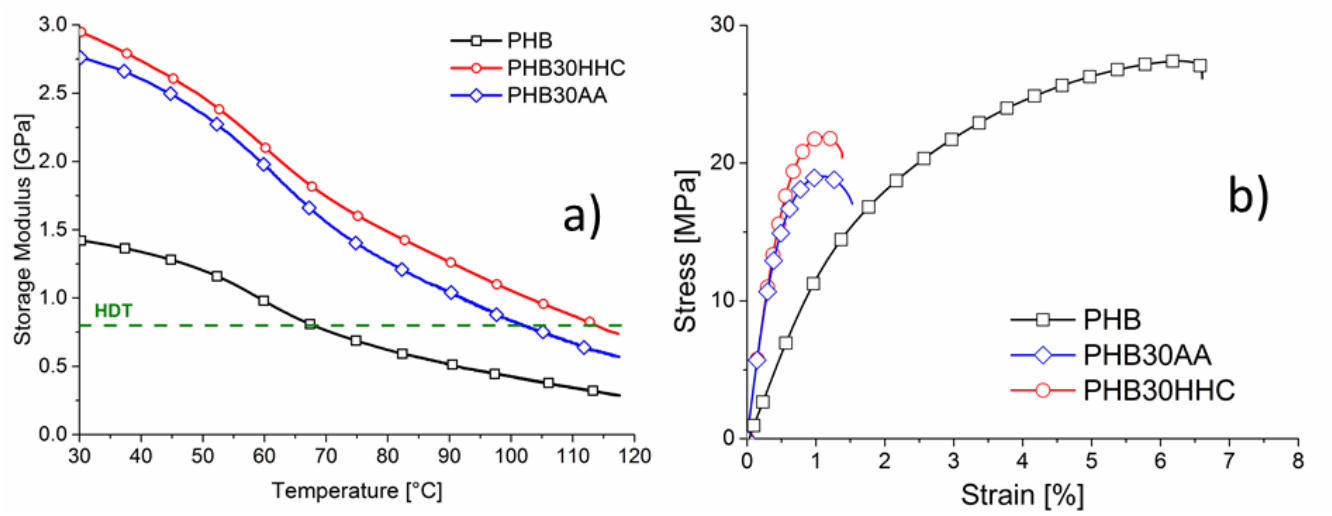

FIG. 3. DMTA curves (a) and representative stress–strain curves from tensile tests (b) of PHB-based composites.

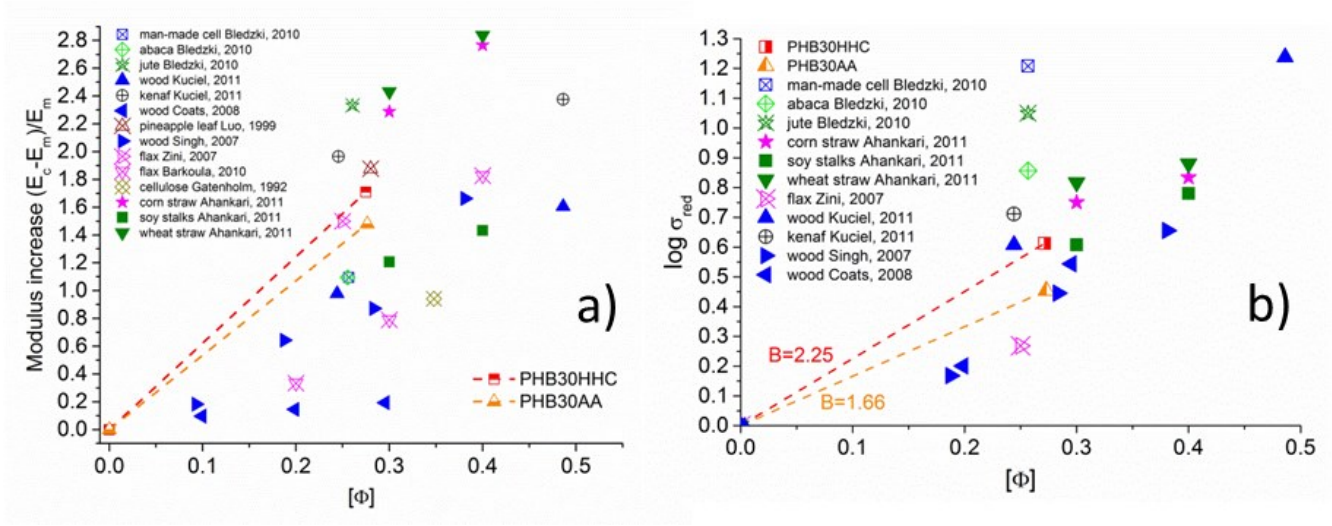

FIG. 4. Modulus increase as a function of volumetric fraction (a) and reduced stress (σred) as a function of the filler volume fraction (Φ) with calculated B factor (b) of PHB-based composites and literature data [25,28, 39, 41, 44].

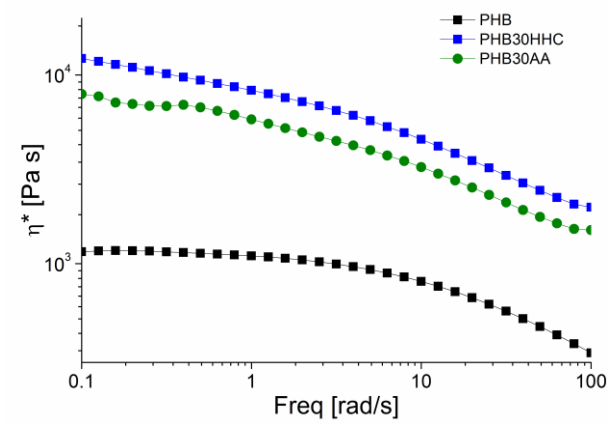

FIG. 5. Complex viscosity (η*) of PHB and PHB-based composites.

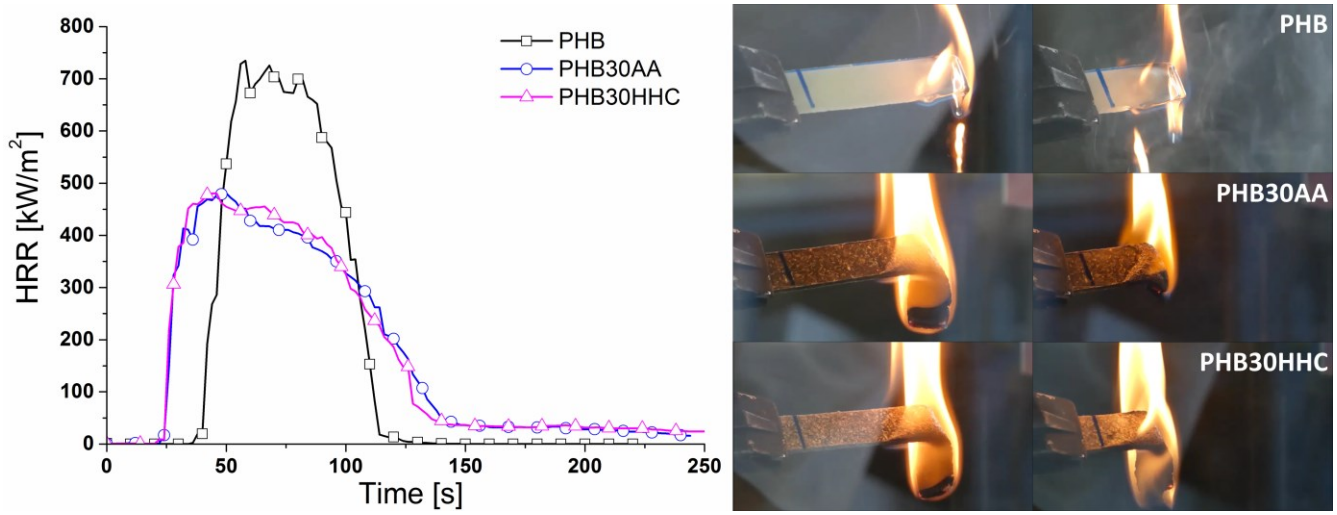

FIG. 6. HRR representative curves and UL 94 HB pictures of PHB and related composites.

Table 1 Percentage of crystallinity and HDT data of PHB-based biocomposites.

Sample	Crystallinity [%]	HDT [°C]
PHB	31	67
PHB30HHC	32	113
PHB30AA	35	102

Table 2 Tension test data of PHB-based composites.

Code	E [GPa]	ΔE [%]*	σ_{max} [MPa]	$\Delta\sigma_{max}$ [%]*	ε [%]	Δε [%]*
PHB	1365 ± 36	-	27.5± 0.4	-	6.7± 0.7	-
PHB30HHC	3703 ± 67	171	22.0± 1.1	-20	1.5± 0.3	-76
PHB30AA	3395 ± 37	148	18.7± 0.4	-32	1.5± 0.3	-76

Table 3 Cone calorimetry and UL94 HB data of PHB and related composites.

Sample code	TTI±d [s]	Mass [g]	PHRR±d [kW/m^2] (%)	THR±d [MJ/m^2]	TSR±d [m^2/m^2]	Residue ±d [%]	FIGRA	UL94 HB BR±d [mm/min]
PHB	45±3	18.3	714±35	39.8±1.3	379±10	0.0±0.1	11.4±1.1	48±7
PHB30AA	29±1	21.5	487±8 (-32)	40.0±0.5	493±7	7.8±0.1	10.9±0.4	29±5
PHB30HHC	30±1	20.9	478±25 (-33)	40.3±0.3	484±37	6.5±0.1	9.6±0.5	38±4

d=standard deviation

References

[1] M. Carus, S. Karst, A. Kauffmann, J. Hobson and S. Bertucelli, *European Industrial Hemp Association (EIHA), Hürth (Germany)*, (2013).

[2] T.-T. Nguyen, V. Picandet, S. Amziane and C. Baley, *European Journal of Environmental and Civil Engineering*, **13**, 1039 (2009).

[3] FAO STAT, (2012).

[4] K.G. Satyanarayana, G.G.C. Arizaga and F. Wypych, *Progress in Polymer Science*, **34**, 982 (2009).

[5] C. Baillie, *Green composites: polymer composites and the environment*, CRC Press, (2005)

[6] G. Bogoeva-Gaceva, M. Avella, M. Malinconico, A. Buzarovska, A. Grozdanov, G. Gentile and M. Errico, *Polymer composites*, **28**, 98 (2007).

[7] M.P.M. Dicker, P.F. Duckworth, A.B. Baker, G. Francois, M.K. Hazzard and P.M. Weaver, *Composites Part A: Applied Science and Manufacturing*, **56**, 280 (2014).

[8] D.B. Dittenber and H.V.S. GangaRao, *Composites Part a-Applied Science and Manufacturing*, **43**, 1419 (2012).

[9] M.A. Fuqua, S.S. Huo and C.A. Ulven, *Polymer Reviews*, **52**, 259 (2012).

[10] T. Gurunathan, S. Mohanty and S.K. Nayak, *Composites Part a-Applied Science and Manufacturing*, **77**, 1 (2015).

[11] A.K. Mohanty, M. Misra and G. Hinrichsen, *Macromolecular Materials and Engineering*, **276**, 1 (2000).

[12] D. Battegazzore, S. Bocchini and A. Frache, *Polymer International*, **65**, 955 (2016).

[13] P.K. Bajpai, I. Singh and J. Madaan, *Journal of Thermoplastic Composite Materials*, **27**, 52 (2014).

[14] D. Battegazzore, S. Bocchini, J. Alongi and A. Frache, *RSC Advances*, **4**, 54703 (2014).

[15] D. Battegazzore, J. Alongi and A. Frache, *Journal of Polymers and the Environment*, **22**, 88 (2014).

[16] L. Danyadi, T. Janecska, Z. Szabo, G. Nagy, J. Moczo and B. Pukanszky, *Composites Science and Technology*, **67**, 2838 (2007).

[17] L.S. Michael Carus, in, European Industrial Hemp Association (EIHA), 2016.

[18] D. Battegazzore, J. Alongi, D. Duraccio and A. Frache, *Journal of Polymers and the Environment*, **26**, 1652 (2018).

[19] D. Battegazzore, J. Alongi, A. Frache, L. Wagberg and F. Carosio, *Materials Today Communications*, **13**, 92 (2017).

[20] S. Panthapulakkal and M. Sain, *Journal of Applied Polymer Science*, **103**, 2432 (2007).

[21] A. Mohanty, P. Tummala, W. Liu, M. Misra, P. Mulukutla and L. Drzal, *Journal of Polymers and the Environment*, **13**, 279 (2005).

[22] G.I. Williams and R.P. Wool, *Applied Composite Materials*, **7**, 421 (2000).

[23] G. Mehta, L.T. Drzal, A.K. Mohanty and M. Misra, *Journal of applied polymer science*, **99**, 1055 (2006).

[24] S. Mishra, J. Naik and Y. Patil, *Advances in Polymer Technology*, **23**, 46 (2004).

[25] A. Bledzki, H.P. Fink and K. Specht, *Journal of Applied Polymer Science*, **93**, 2150 (2004).

[26] T. Behzad and M. Sain, *Polymers and Polymer Composites*, **13**, 235 (2005).

[27] M. Ragoubi, D. Bienaimé, S. Molina, B. George and A. Merlin, *Industrial Crops and Products*, **31**, 344 (2010).

[28] S. Mishra and J. Naik, *Journal of applied polymer science*, **68**, 681 (1998).

[29] K.L. Pickering, M.G.A. Efendy and T.M. Le, *Composites Part A: Applied Science and Manufacturing*, **83**, 98 (2016).

[30] S. Kuciel and A. Liber-Kneć, *Polimery*, **56**, 218 (2011).

[31] S. Luo and A. Netravali, *Polymer composites*, **20**, 367 (1999).

[32] V. Nagarajan, A.K. Mohanty and M. Misra, *ACS Sustainable Chemistry & Engineering*, **1**, 325 (2013).

[33] E. Zini, M.L. Focarete, I. Noda and M. Scandola, *Composites Science and Technology*, **67**, 2085 (2007).

[34] P. Barham, A. Keller, E. Otun and P. Holmes, *Journal of Materials Science*, **19**, 2781 (1984).

[35] ISO 5660.

[36] L. Nicolais and M. Narkis, *Polymer Engineering & Science*, **11**, 194 (1971).

[37] B. Pukanszky, *Composites*, **21**, 255 (1990).

[38] B. Turcsanyi, B. Pukanszky and F. Tüdõs, *Journal of Materials Science Letters*, **7**, 160 (1988).

[39] J. Móczó and B. Pukánszky, *Journal of Industrial and Engineering Chemistry*, **14**, 535 (2008).

[40] A. Dorigato, M. Sebastiani, A. Pegoretti and L. Fambri, *Journal of Polymers and the Environment*, **20**, 713 (2012).

[41] A. Lazzeri and V.T. Phuong, *Composites Science and Technology*, **93**, 106 (2014).

[42] D. Battegazzore, A. Noori and A. Frache, *Journal of Composite Materials*, (2018) DOI: 002199831879131.

[43] M.T. Takemori, *Polymer Engineering and Science*, **19**, 1104 (1979).

[44] S. Singh and A. Mohanty, *Composites Science and Technology*, **67**, 1753 (2007).

[45] A. Bledzki and A. Jaszkiewicz, *Composites science and technology*, **70**, 1687 (2010).

[46] S.S. Ahankari, A.K. Mohanty and M. Misra, *Composites Science and Technology*, **71**, 653 (2011).

[47] P. Gatenholm, J. Kubat and A. Mathiasson, *Journal of Applied Polymer Science*, **45**, 1667 (1992).

[48] N. Barkoula, S. Garkhail and T. Peijs, *Industrial Crops and Products*, **31**, 34 (2010).

[49] E.R. Coats, F.J. Loge, M.P. Wolcott, K. Englund and A.G. McDonald, *Bioresource Technology*, **99**, 2680 (2008).

[50] S. Kuciel and A. Liber-Knec, Polimery, **56**, 218 (2011).

[51] O.O. Fadiran, N. Girouard and J.C. Meredith, *Emergent Materials*, **1**, 95 (2018).

[52] D. Battegazzore, A. Frache and F. Carosio, *Acs Sustainable Chemistry & Engineering*, **6**, 9601 (2018).

[53] D. Battegazzore, A. Frache, T. Abt and M.L. Maspoch, *Composites Part B-Engineering*, **148**, 188 (2018).

[54] J. Zhu, H. Zhu, K. Immonen, J. Brighton and H. Abhyankar, *Industrial Crops and Products*, **67**, 346 (2015).

[55] A. Gupta, W. Simmons, G.T. Schueneman, D. Hylton and E.A. Mintz, *ACS Sustainable Chemistry & Engineering*, **5**, 1711 (2017).

[56] B. Schartel, M. Bartholmai and U. Knoll, *Polymers for Advanced Technologies*, **17**, 772 (2006).

[57] R. Kozłowski and M. Władyka-Przybylak, *Polymers for Advanced Technologies*, **19**, 446 (2008).

[58] B. Schartel and T.R. Hull, *Fire and Materials*, **31**, 327 (2007).

[59] L. Costes, F. Laoutid, S. Brohez and P. Dubois, *Materials Science and Engineering: R: Reports*, **117**, 1 (2017).

[60] K.M. Zadeh, D. Ponnamma and M. Al Ali Al-Maadeed, *Polymer Testing*, **61**, 341 (2017).

[61] D. Battegazzore, J. Alongi, D. Duraccio and A. Frache, *Journal of Polymers and the Environment*, **26**, 3731 (2018).

[62] M.E. Mngomezulu, M.J. John, V. Jacobs and A.S. Luyt, *Carbohydr Polym*, **111**, 149 (2014).

[63] N. Ayrilmis, S. Jarusombuti, V. Fueangvivat, P. Bauchongkol and R.H. White, *Fibers and Polymers*, **12**, 919 (2011).

[64] S. Chapple and R. Anandjiwala, *Journal of Thermoplastic Composite Materials*, **23**, 871 (2010).

[65] Z.N. Azwa, B.F. Yousif, A.C. Manalo and W. Karunasena, *Materials & Design*, **47**, 424 (2013).